PHILOSOPHICAL TRANSACTIONS OF THE ROYAL SOCIETY B BIOLOGICAL SCIENCES

N.m.r. Imaging of Intact Biological Systems

E. R. Andrew

Phil. Trans. R. Soc. Lond. B 1980 **289**, 471-481
doi: 10.1098/rstb.1980.0065

Phil. Trans. R. Soc. Lond. B **289**, 471–481 (1980) [471]
Printed in Great Britain

N.m.r. imaging of intact biological systems

By E. R. Andrew
Department of Physics, University of Nottingham, University Park, Nottingham NG7 2RD, U.K.

[Plates 1 and 2]

Internal images of structured objects may be obtained with n.m.r. by labelling component parts with different magnetic field strengths and therefore recognizably different n.m.r. frequencies. A linear field gradient generates a one-dimensional projection of nuclear density and a variety of techniques are employed to manipulate this one-dimensional probe to yield internal images in two and three dimensions.

In the past few years, n.m.r. imaging, sometimes also called zeugmatography or spin mapping, has been applied progressively to provide proton images of small phantoms, fruit, vegetables and small animals, and finally to *in vivo* imaging of the human body; it promises to provide a valuable means of interior investigation of intact biological systems generally. For medical imaging the method is non-invasive, does not use ionizing radiations, appears to be without hazard and penetrates bony cavities without attenuation. Furthermore, other n.m.r. parameters, for example, relaxation times and fluid flow, may also be mapped; there is evidence that the relaxation times from tumours are significantly longer than those from corresponding normal tissue. Effort to date has mostly been concentrated on proton n.m.r., but some work has been done with other nuclei.

Three examples are shown of n.m.r. images of intact biological systems: a fruit, an animal and a human system. The discussion includes the quantitative nature of the images, tissue discrimination, the relation between resolution in the image and image acquisition time, attenuation and phase shift of the r.f. field in the biological tissue, and magnets suitable for n.m.r. imaging. In principle, all conventional n.m.r. techniques can be combined with n.m.r. imaging methods in order to investigate heterogeneous systems. Overhauser imaging is briefly discussed.

Introduction

The use of nuclear magnetic resonance (n.m.r.) to provide images of intact biological systems is a relatively recent development in n.m.r., and one that, in a literal sense, can be said to add new dimensions to the subject. My purpose in this paper is to provide an introduction to n.m.r. imaging, particularly to those participants in the Discussion Meeting who are less familiar with this subject.

Previous papers at this meeting have been concerned with high resolution n.m.r. spectroscopy of small biological specimens, typically 10 mm in size, examined in very uniform magnetic fields, homogeneous to one part in 10^9. The specimens were cells or organs and were not strongly structured on a macroscopic scale. In this and following papers in this Discussion, we are concerned with whole organisms, vegetable, animal and human; they are not small, but are typically 50–500 mm in diameter, they are highly structured and heterogeneous and we are particularly concerned to investigate and display their structures.

In n.m.r. imaging, the specimen is placed in a deliberately non-uniform magnetic field, whose purpose is to label different parts of the specimens with different Zeeman field strengths. The nuclei in these parts therefore respond with recognizably different n.m.r. frequencies, so enabling the structure to be determined.

The subject has acquired a variety of names, the most common being n.m.r. imaging, spin mapping and zeugmatography. The first of these is self-explanatory. The second name (Hinshaw 1974*a*, *b*) recognizes that an n.m.r. image is a map of nuclear spin density and related parameters. The intriguing name zeugmatography, proposed by Lauterbur (1973), comes from the Greek work *zeugma* (that which joins together) and recognizes the necessity of joining together in the object a spatially defining inhomogeneous field with the resonant n.m.r. electromagnetic field in order to generate the image. When used in a medical context, the name n.m.r. tomography has been suggested.

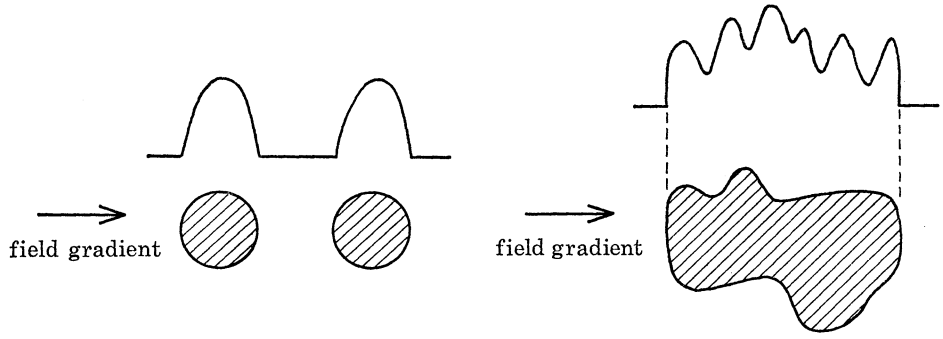

FIGURE 1. This diagram illustrates how the application of a linear field gradient to an object generates an n.m.r. spectrum that is a one-dimensional projection of mobile proton density along the gradient direction. **Left:** two tubes of water. **Right:** a general, irregularly shaped object.

METHODS

Biological systems provide strong proton n.m.r. signals, particularly from water, fat and other fluid or soft components. Professor Felix Bloch (1978) carried out the first biological n.m.r. experiment very soon after the discovery of n.m.r., when he placed his finger in the probe coil of the first nuclear induction equipment (Bloch *et al.* 1946), and obtained a strong proton n.m.r. signal. It was, however, an integrated signal from the protons in the blood, tissue, fat, bone marrow and other components of the finger and it provided no spatial information.

The intrinsic n.m.r. line width of the strongly responding biological components is narrow, typically a few Hz. If, therefore, a linear magnetic field gradient of the order of 10^{-2} T m^{-1} is superposed on the usual highly uniform laboratory magnetic field, the n.m.r. spectrum provides a one-dimensional (1D) profile or projection of proton density along the direction of the gradient. This is illustrated in figure 1 for two tubes of water and for a general, irregularly shaped object with an arbitrary internal distribution of mobile protons.

Such n.m.r. 1D projections are not new and had been investigated some years ago, with simple glass and liquid structures, by Gabillard (1951, 1952) (see also Andrew 1955), who also studied their dynamic response. Field gradients are also an essential feature of the study of molecular diffusion in fluids by the spin echo method (Hahn 1950), in methods of information storage (Anderson *et al.* 1955, Andrew *et al.* 1970) and in the investigation of periodic structures by the n.m.r. 'diffraction' method (Mansfield & Grannell 1973).

For an image or picture, one requires at least a two-dimensional (2D) representation of nuclear density. Better still, one would like to have a 2D image of a thin, defined plane in the object; a stack or set of such images of coplanar slices in the object then provides a complete three-dimensional (3D) representation of the object.

PHILOSOPHICAL TRANSACTIONS OF THE ROYAL SOCIETY B BIOLOGICAL SCIENCES

The first proposal of an n.m.r. imaging idea was provided by Damadian (1972), in a patent application, and the first practical realization of a 2D n.m.r. image came from Lauterbur (1973). By applying the gradient along a number of different directions relative to the object, a number of different 1D profiles are obtained, these may be combined by computer to give a 2D projection image of the object. The method is closely similar to the projection–reconstruction procedures used in computer tomographic (c.t.) X-ray scanning, pioneered by Hounsfield (1973).

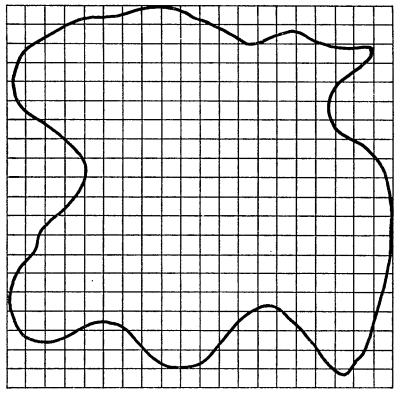

FIGURE 2. The image of any object may be divided into an $n \times n$ matrix of picture elements (pixels).

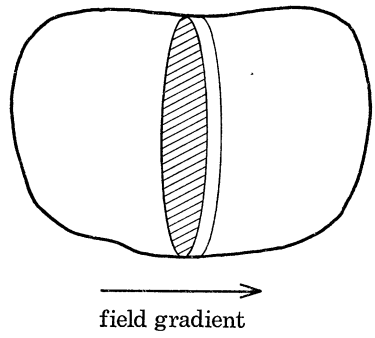

FIGURE 3. An imaging plane defined in the object.

In general, we can divide our object and its 2D image into an $n \times n$ matrix of picture elements (pixels), as illustrated in figure 2, and we need to find the n.m.r. response, a_{pq}, from each of the n^2 matrix elements. If each 1D projection consists of n data values, each of which is a sum, Σa_{pq}, of n elements, and, if n different projections are obtained, we have n^2 simultaneous equations in the n^2 unknown quantities, a_{pq}; by computer, these may be solved by iterative procedures, or by back projection, or other methods (Pullan *et al.* 1976; Pullan 1979), to generate an image of $n \times n$ picture elements.

In c.t. X-ray scanning, the narrow pencil beams of X-ray define a thin imaging slice. In n.m.r. imaging, the whole object within the n.m.r. probe coil is irradiated, and the method as so far described does not provide a thin imaging plane; the resulting image is therefore a 2D projection image onto a plane normal to the axis about which the gradient directions are rotated. For an object structured in all three dimensions, such 2D projection images do not suffice. In this situation, the projection–reconstruction approach may be extended by dividing the object into $n \times n \times n$ cuboidal volume elements (voxels); one must now apply the gradient isotropically from n^2 directions, to yield n^3 equations in n^3 unknowns. Since to obtain good resolution in the image usually requires $n > 100$, there is now a very large computing problem.

Although this 3D computing exercise has in one case been successfully attempted with $n = 60$ (Lauterbur *et al.* 1977), the problem is usually circumvented by methods that define a thin imaging slice in the object (figure 3). In one method (Hinshaw 1974*a*, *b* 1976), the field gradient, g, is caused to alternate at a low frequency, Ω, so defining a zero field plane of approximate thickness 2Ω in terms of frequency, or $2\Omega/\gamma g$ (γ, the magnetogyric ratio) in terms of length. In another method (Garroway *et al.* 1974; Lauterbur *et al.* 1974; Hutchison 1976), a thin plane in the object is selectively excited in a static field gradient by a pulse sequence whose spectrum is carefully tailored to correspond to the thin band of resonance frequencies in this plane.

PHILOSOPHICAL TRANSACTIONS OF THE ROYAL SOCIETY B BIOLOGICAL SCIENCES

A thin plane in the object having been defined by one of these methods, an n.m.r. image of the plane may be obtained in one of several ways. One way is to apply the projection–reconstruction method to the plane, a linear gradient being applied in a number of directions in the plane (Lauterbur *et al.* 1974; Brooker & Hinshaw 1978). Alternatively, the same procedures used for defining the plane, namely an alternating gradient or selective irradiation, may now be used to define a strip in the plane. If now a static gradient is applied along the strip and a free induction decay is recorded, its Fourier transform yields the proton distribution along the strip. The strip may be advanced electronically to scan the defined plane, and the image displayed synchronously on an oscilloscope (Mansfield *et al.* 1976; Hinshaw 1976; Andrew *et al.* 1977). Yet another approach is to apply the principles of 2D Fourier transform n.m.r. spectroscopy to image the defined plane (Kumar *et al.* 1975*a*, *b*; Brunner & Ernst 1979).

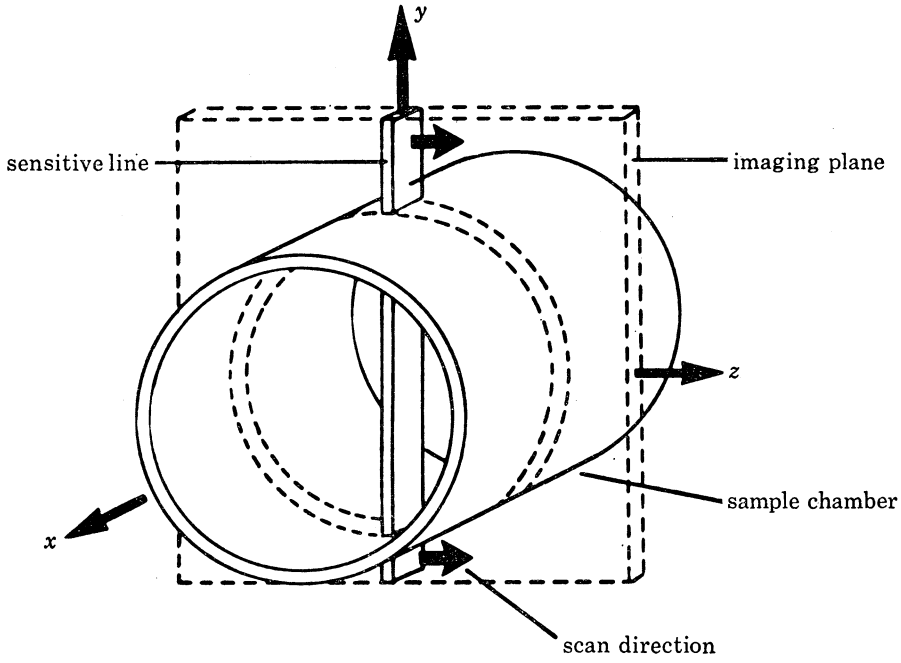

FIGURE 4. Sample chamber used for obtaining the n.m.r. images shown in plates 1 and 2. The sensitive line scans through the defined plane in the specimen during the formation of an image. The chamber is a glass tube of 8 cm diameter on which the r.f. coil is wound, and is mounted transversely in the gap of the electromagnet, which applies a magnetic field along the *z*-direction.

It will be noticed that all these approaches have one feature in common. They recognize that a linear field gradient is essentially a 1D probe of investigation; to yield 2D or 3D information, time-dependence must be introduced, either by modulating the gradient, or by switching it, or by both of these means.

This short introduction to methods of imaging by no means exhausts the approaches that are possible. Two other basic methods that must be mentioned are the FONAR method (Damadian *et al.* 1976) and the rotating frame zeumatography method (Hoult 1979). Combinations that exploit the best features of the various methods are possible, and refinements that achieve rapid scans have been developed (Mansfield 1977). More detailed reviews of the methods have been given elsewhere (Andrew 1976; Mansfield 1976; Brunner & Ernst 1979).

PHILOSOPHICAL TRANSACTIONS OF THE ROYAL SOCIETY B BIOLOGICAL SCIENCES

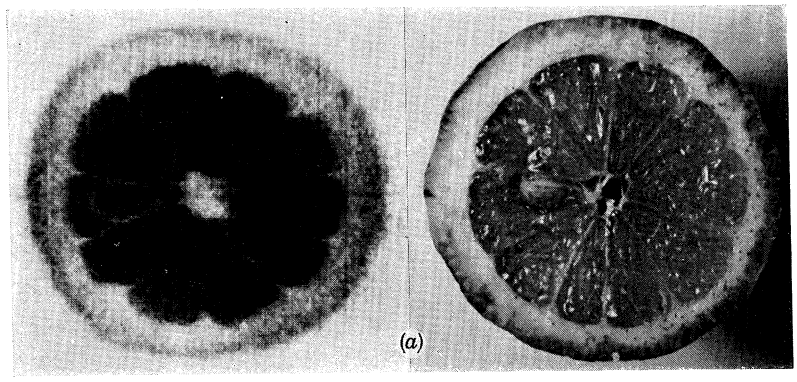

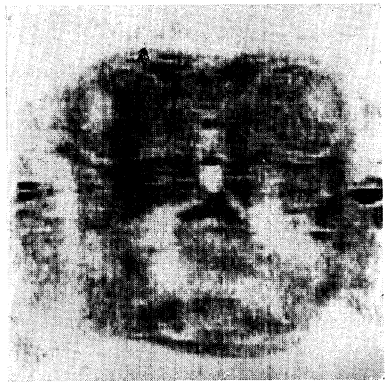

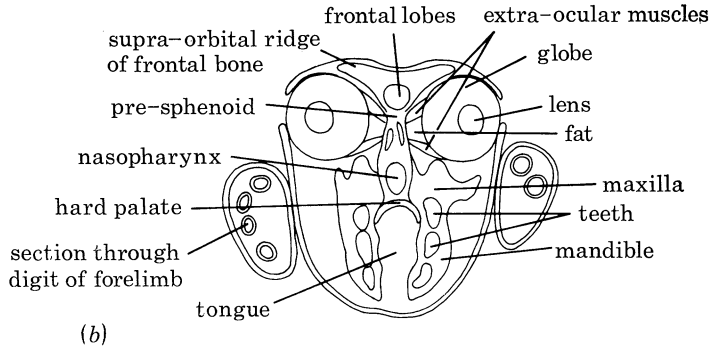

FIGURE 5. (*a*) Thin transverse section proton n.m.r. image of an intact lemon (left) and photograph of actual section cut subsequently (right). (*b*) Thin coronal section proton n.m.r. image through middle of orbits of rabbit's head (left) and annotated diagram indicating recognizable anatomical structure (right). Details of these images are given in the text. The images in plates 1 and 2 were obtained by an MRC supported group at Nottingham University consisting of E. R. Andrew, P. A. Bottomley, W. S. Hinshaw, G. N. Holland, W. S. Moore, C. Simaroj & B. S. Worthington.

(*Facing p.* 474)

PHILOSOPHICAL TRANSACTIONS OF THE ROYAL SOCIETY B BIOLOGICAL SCIENCES

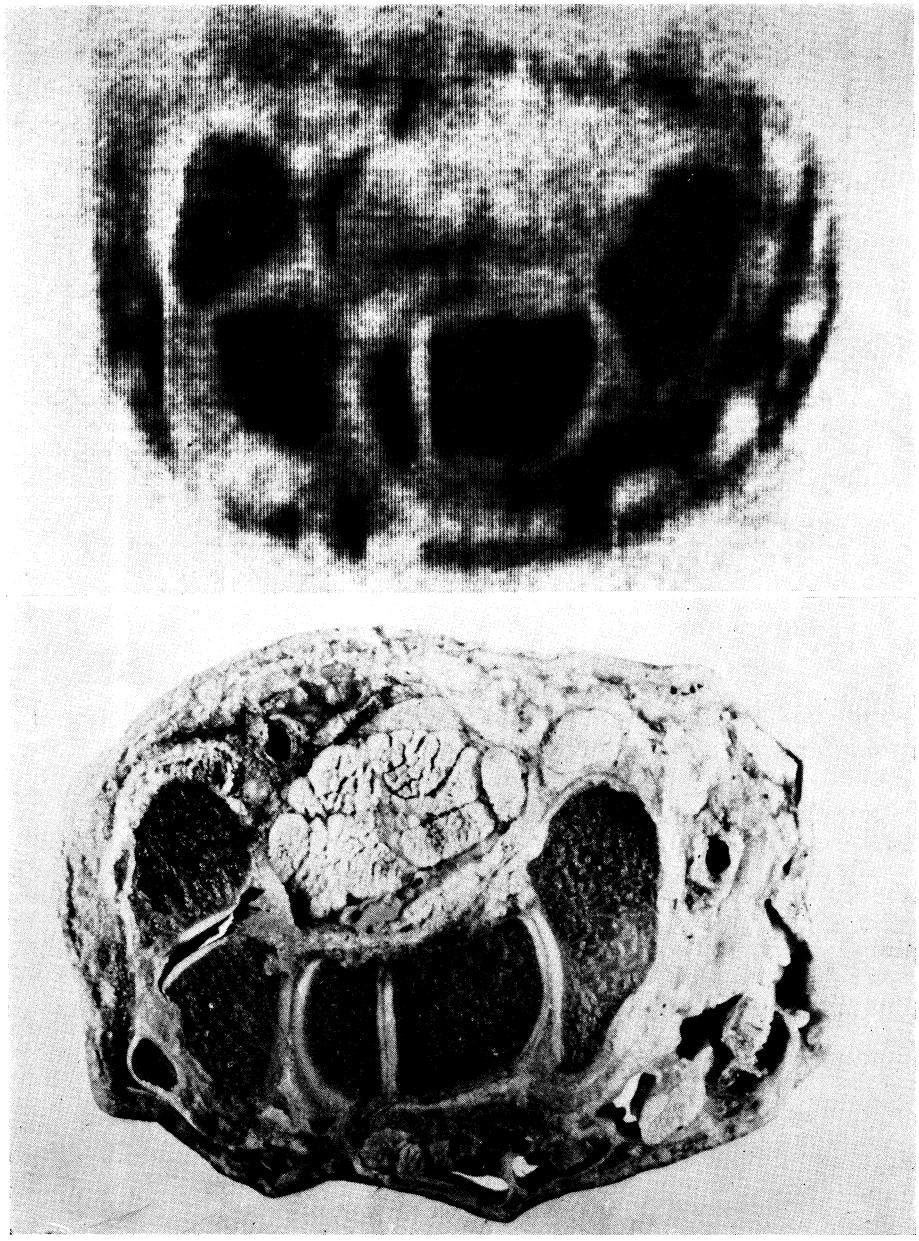

FIGURE 6. Thin transverse proton n.m.r. image through the left wrist of Dr P. Bottomley (above) and a photograph of a matching section from a cadaver wrist (below). Details of the image and the anatomical features observable are described in the text (Hinshaw *et al.* 1977, 1978*b*).

PHILOSOPHICAL TRANSACTIONS OF THE ROYAL SOCIETY B BIOLOGICAL SCIENCES

Images

As an illustration of the quality and resolution that can be obtained in n.m.r. images of intact biological systems, examples from our laboratory are shown in figures 5 and 6 (plates 1, 2). The three examples shown are of a fruit, an animal, and a human system. The images were obtained by the multiple sensitive point method (Hinshaw 1976; Andrew *et al.* 1977; Hinshaw *et al.* 1978*a*, *b*), in which the imaging plane is defined by an alternating field gradient, and strips in this plane are successively defined by an orthogonal alternating gradient, as illustrated in figure 4. The images have a 128×128 pixel array, interpolated to 256×256, and were recorded in 5 to 15 min. The thickness of the imaging plane was 3 mm and the resolution in the images is about 0.5 mm. The Zeeman field was 0.7 T and the proton n.m.r. frequency was 30 MHz. The n.m.r. signal was recorded on a sixteen level intensity scale.

The proton n.m.r. image in figure 5*a* is of an intact lemon and alongside is shown a photograph of the actual section, cut after the lemon had been imaged. The diameter of the lemon was 7 cm. Strong n.m.r. signals were recorded from the fluid in the lemon segments; a weaker signal was recorded from the skin. The hard septum planes yield little signal and were well resolved. The pip seen in the photograph of this section is clearly reproduced in the image, its hard casing giving a bright outline. The oily layer just under the surface of the skin of the lemon gives a rather stronger signal than the dry pithy layer beneath (Andrew *et al.* 1979).

The image in figure 5*b* is of a thin coronal section of a rabbit's head, one of a series of such sections (Hinshaw *et al.* 1978*a*). The head was subsequently cast in plaster and sectioned at 1 cm intervals for comparison and identification with the corresponding n.m.r. images. The main features are illustrated in the accompanying diagram. The aqueous and vitreous humour of the eyes shows strongly, contrasting with the weak signal from the more solid lenses. The hard outer sclerotic coating of the eyes is exhibited as white rings enclosing them. Also visible in this cross section are the frontal lobe of the brain, the nasal cavity, the palate and the tongue. There is good geometric correspondence with the actual section.

The proton n.m.r. image in figure 6 is of a thin transverse section through the left wrist of Dr P. Bottomley. The proton signal from the subcutaneous tissue and fat defines the margin. Prominently featured are the five carpal bones (from left to right): pisiform, triquetrum, capitate, lunate and scaphoid. The strong signals evidently come from the marrow and fat within the bones; the hard cortical bone casing generates the surrounding light regions. A photograph of a matching section from a cadaver arm is also shown, illustrating the features visible in the image. Light patches punctuating the subcutaneous tissue on the dorsal side arise from the harder extensor tendons. The ulnar and radial arteries and some veins are also visible (Hinshaw *et al.* 1977, 1978*b*).

These three examples of n.m.r. images are shown here in black and white. They may also be displayed in colour, and an example of a transverse abdominal section of an intact rat was shown in the lecture (Andrew *et al.* 1977; Holland & Bottomley 1977). Advantages of the use of colour are the greater number of colours that the eye can discriminate than grey levels, and the use of colour to display an orthogonal parameter such as relaxation time or flow velocity, while retaining intensity as a measure of n.m.r. signal strength.

PHILOSOPHICAL TRANSACTIONS OF THE ROYAL SOCIETY B BIOLOGICAL SCIENCES

Discussion

The examples of n.m.r. images shown in the previous section serve to illustrate a number of general features of n.m.r. imaging, which will now be considered in turn.

1. *Nature of the image*

It is first of all important to ask what is actually being displayed in the n.m.r. image. The image is not just a 2D representation of proton density $\rho(x, y, z)$ at each point, x, y, z, in the defined slice of the object. Rather, it is a spatial representation of the n.m.r. signal. The n.m.r. signal is certainly proportional to the proton density at each point, since the nuclear magnetization at each point is proportional to the proton density. In general, the n.m.r. signal from the volume element at x, y, z will be given by

$$[\rho f(T_1, T_2, v, \ldots)]_{xyz},$$

the precise form of the function, f, of the relaxation times, T_1, T_2, and of the fluid flow, v, and other parameters, depending on the details of the method of measurement. Under driven conditions it may approximate to

$$[\rho T_2/T_1]_{xyz}.$$

For fluids and soft tissues, T_1 and T_2 are approximately equal and the n.m.r. signal is a measure of ρ. For solids, $T_2 \ll T_1$ and the n.m.r. response is weak. This provides an explanation of the tissue discrimination observed in the animal and human images. Strong signals are obtained from fluids, fats and solft tissues, intermediate signals from tendon and muscle and other tissues, depending on their 'hardness', weak signals from teeth, cortical bone casing and voids. Particular parameters such as T_1 may be studied or imaged by examination of the dynamic response of the n.m.r. signal.

2. *Resolution and time*

It is important to note that there is a close relation between the resolution in the image and the time taken to acquire the image. If it is desired to improve the resolution by, say, a factor of two in all three dimensions, each voxel is reduced in volume by a factor of eight. If all other parameters are kept constant, the time required to obtain an n.m.r. signal of the same signal to noise ratio as before is therefore increased by a factor of 64. In fact, the imaging time increases as n^6. If it is merely desired to improve the resolution in the image plane, while retaining the same plane thickness, the picture time increases only as n^4. In either case one pays dearly in acquisition time for much improved resolution.

It is clear, therefore, that the efficient gathering of n.m.r. information is of prime importance if imaging times are to be reduced substantially without sacrifice of signal to noise ratio or resolution (Brunner & Ernst 1979).

3. *Radio frequency penetration*

Biological tissues are moderate electrical conductors and we should therefore expect some attenuation of the electromagnetic radiation at the n.m.r. frequency as it penetrates the intact biological systems. No significant attenuation was observed in the examples shown in figures 5 and 6, and evidently the dimensions of these objects are less than the radio frequency skin depth at 30 MHz. However, this effect could be more important for whole body human imaging. We have therefore made calculations (Bottomley & Andrew 1978) of the attenuation

and phase shift of electromagnetic radiation in the body as a function of frequency between 1 and 100 MHz. As a model of the human body we took a homogeneous cylinder of radius 0.2 m. Figure 7 shows the variation with frequency of the radio frequency magnetic field on the cylinder axis, and also of the phase on the axis, for a variety of tissue impedances.

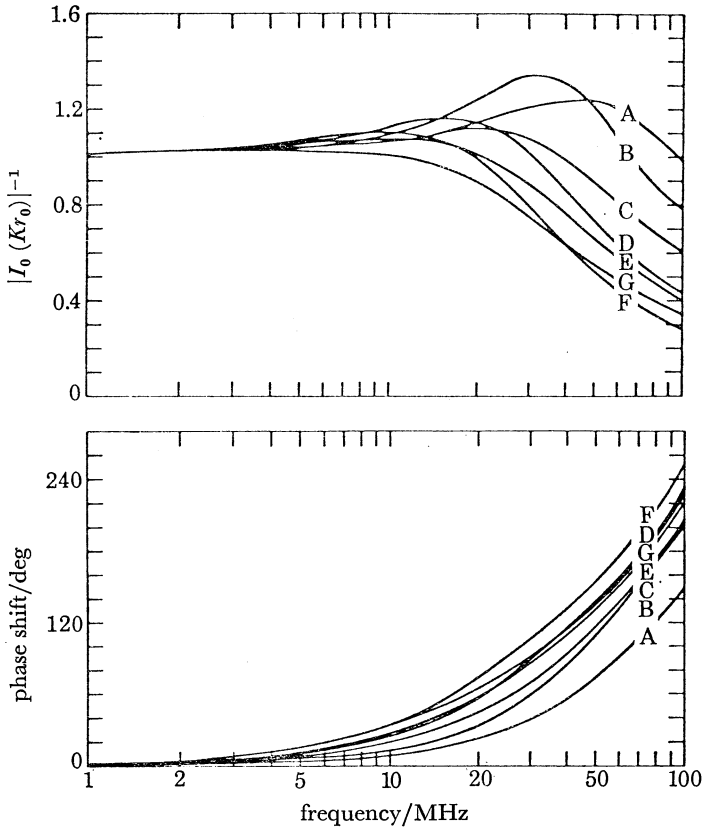

FIGURE 7. Variation with frequency of the r.f. magnetic field (upper diagram) and phase (lower diagram) on the axis of homogeneous tissue cylinders of radius 0.2 m. The curves have been calculated by means of measured impedances of the various rat tissues indicated (Bottomley & Andrew 1978). A, lung; B, brain; C, liver; D, kidney; E, heart; F, tumour; G, muscle.

It is seen that significant attenuation and phase distortion occur above 10 MHz. (For the objects of intermediate size, imaged in figures 5, 6, the corresponding frequency is of order 100 MHz, which explains the lack of attenuation encountered.) If attenuation and phase shift are to be avoided in proton n.m.r. imaging of the whole human body the laboratory magnetic field should therefore not exceed 0.2 T. For parts of the human body of smaller cross section, such as the head and limbs, higher fields and frequencies may be acceptable, as also for cross-sections containing significant voids such as the chest. It may in any case be worthwhile to work in higher field strengths in order to enjoy the resulting higher n.m.r. sensitivity, accepting the need to make corrections for attenuation and phase errors.

4. *Magnets*

For biological systems of the order of 10 cm in size it is possible to use modified versions of the types of iron electromagnet used in conventional n.m.r. spectroscopy. On the other hand, in order to carry out n.m.r. imaging on the whole human body, magnets with a much larger

PHILOSOPHICAL TRANSACTIONS OF THE ROYAL SOCIETY B BIOLOGICAL SCIENCES

working volume are required. A common configuration is depicted in figure 8. It consists of four coils approximating to a 'spherical' configuration. Standing 2 m high, it has an access of 60 cm through the end coils to take a horizontal patient. Such magnets generate fields of 0.1 T with about 20 kW of power. As discussed in the previous section, with such field strengths problems of radio frequency attenuation and phase shift should be absent. At the time of writing, at least six magnets of this general form of construction are now known to be in use.

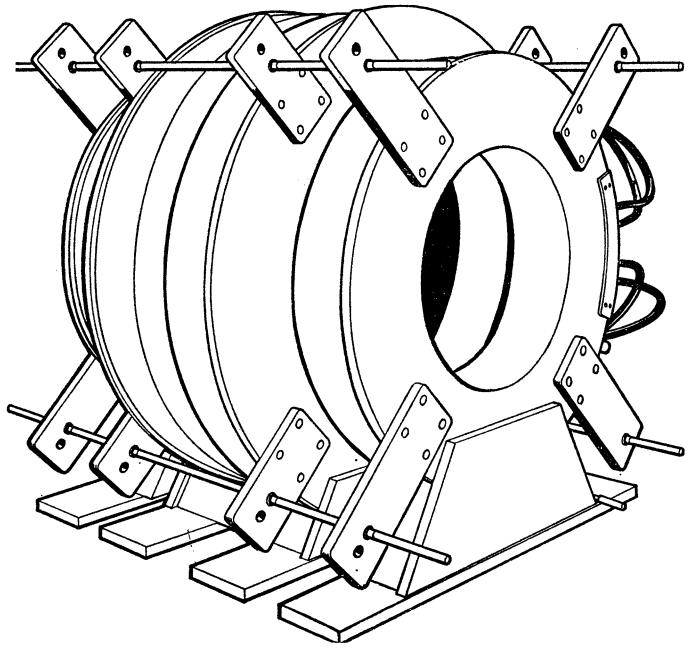

FIGURE 8. A four coil, air core, water cooled, resistive electromagnet for human whole body n.m.r. imaging.

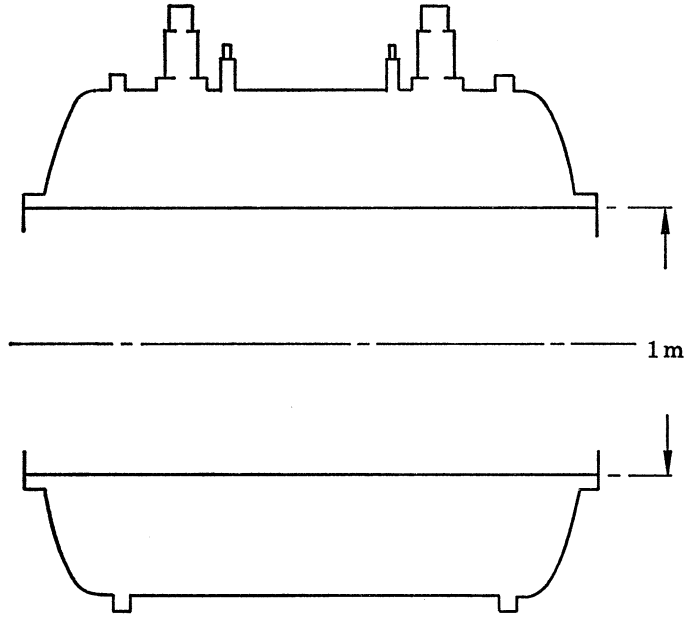

FIGURE 9. A large bore superconducting magnet for human whole body n.m.r. imaging.

PHILOSOPHICAL TRANSACTIONS OF THE ROYAL SOCIETY B BIOLOGICAL SCIENCES

Large superconducting magnets are now available commercially for whole body n.m.r. imaging and an example is shown in figure 9. It has a straight-through horizontal bore of about 1 m diameter, stands about 2 m high and produces magnetic fields up to 2 T; liquid helium consumption is about 10 l per day.

Iron core electromagnets could, in principle, be used for whole body imaging, but it seems doubtful that they offer any advantage. Spare magnets capable of modification for imaging stand idle in particle physics laboratories, but they tend to be extremely massive, with large appetites for power and water.

5. *Hazard*

There is a substantial literature on biological effects of magnetic fields. Scientific workers have been exposed to fields up to 2 T and have inserted their heads into energized cyclotron magnets. There have been no noticeable ill effects, other than sensations in the mouth, attributed to e.m.fs generated in metal fillings in the teeth when the head is moved in a magnetic field. So far no volunteer who has been imaged by n.m.r., whether of the head, chest, abdomen, arms or hands has reported any significant effects. Nevertheless, this is not a well charted area, and is one in which we should surely proceed with caution on human subjects.

Some imaging systems use alternating or rapidly switched magnetic field gradients. Here again no ill effects have been reported, but there is less evidence and more reason to be careful on account of possible effects on the nervous system, the brain and the heart.

Many years of application of short wave diathermic treatment to various parts of the body, including the back, neck and head, have revealed no important hazard in the proper application of the electromagnetic radiation to the parts of the body to be treated. Although peak power levels in n.m.r. imaging may be at the kilowatt level, typical mean power levels are only a few watts, two orders of magnitude lower than those used in diathermic therapy. In Britain a 'Government Code of Practice' restricts mean radio frequency exposure of personnel to 10 mW cm^{-2} continuously and to 50 mW cm^{-2} for short periods. Exposures during n.m.r. imaging are expected to be below these recommended levels.

Concluding remarks

Finally, let us give consideration to the possible advantages that n.m.r. may offer as a method of imaging.

First of all, in comparison with other established methods of medical imaging, such as X-ray c.t. scanning, will n.m.r. tomography be cheaper? For whole body human imaging the answer to this question is not at all clear. On the other hand, smaller equipment for specific applications on hands and arms and breasts could well be substantially cheaper. Equipment for examining small animals and other intact biological systems should also be economical, as also in applications to the examination of food products or indeed any other non-metallic opaque objects.

Whatever may be the ultimate answer on costs, there seem to be a number of positive advantages of n.m.r. tomography to which attention may be drawn.

1. As a method of medical examination of the human body it is non-invasive. It does not involve the use of ionizing radiation. It is probably without hazard.

2. The electromagnetic radiation penetrates bony tissue, for example, into the brain, the spinal canal and the marrow of bones, without significant attenuation.

PHILOSOPHICAL TRANSACTIONS OF THE ROYAL SOCIETY B BIOLOGICAL SCIENCES

3. The method measures the density distribution of hydrogen, the most abundant chemical element in human and biological systems, and does so with useful tissue discrimination.

4. Besides measuring proton density, the method can also measure other n.m.r. parameters, such as T_1, T_2, flow and diffusion, in selected regions of the object. This has considerable practical significance since, as Damadian (1971) first indicated, there is evidence that cancerous tissue has significantly longer proton relaxation times than the corresponding normal tissue. Such differences may prove to have important diagnostic value.

Protons have been the favourite nuclei for n.m.r. imaging to date on account of their very favourable n.m.r. characteristics coupled with the high concentration of hydrogen in biological systems. Nevertheless, other nuclei are of interest for n.m.r. imaging. Some n.m.r. imaging has been done with ^{19}F (Holland *et al.* 1977) and may have importance in conjunction with fluorinated pharmaceuticals and with fluorocarbon blood substitutes. A fairly abundant species in all biological systems is ^{31}P, and some phantom images have been obtained (Hoult 1979). Other nuclei that may in due course be of interest are ^{2}H, ^{13}C, ^{14}N, ^{15}N, ^{23}Na.

In principle, the whole range of n.m.r. measurements and techniques with all its variations and refinements as practised conventionally on small homogeneous specimens may now be extended and applied in n.m.r. imaging, enabling them to be carried out at a selected region of a structured heterogeneous system, and mapped in 2D and 3D to give images of all n.m.r. properties and parameters. Thus, as an example, it is possible to combine n.m.r. imaging with high resolution n.m.r. spectroscopy to map the spatial distribution of particular chemical species in a system (Lauterbur *et al.* 1975; Lauterbur, this conference).

Another example that I may suggest is the use of Overhauser enhancement of n.m.r. images by e.s.r. irradiation of paramagnetic molecules that are either normally present in the human or biological system, or that may be introduced as spin labelled pharmaceuticals or otherwise. Good Overhauser enhancement will substantially reduce the image time of all protons interacting with the paramagnetic species. If such species were introduced into the biological system, they would act as tracers and contrast media, standing out strongly against the background of weak unenhanced proton n.m.r. signals from the remainder of the system.

References (Andrew)

Anderson, A. G., Garvin, R. L., Hahn, E. L., Horton, J. W., Tucker, G. L. & Walker, R. M. 1955 Spin echo serial storage memory. *J. appl. Phys.* **26**, 1324–1338.

Andrew, E. R. 1955 *Nuclear magnetic resonance*, p. 135. Cambridge: University Press.

Andrew, E. R. 1976 Zeugmatography. *Proc. IV Ampere International Summer School* (*Pula, Yugoslavia*) (ed. R. Blinc & G. Lahajnar), pp. 1–39. Ljubljana: University of Ljubljana.

Andrew, E. R., Bottomley, P. A., Hinshaw, W. S., Holland, G. N., Moore, W. S. & Simaroj, C. 1977 NMR images by the multiple sensitive point method: application to larger biological systems. *Phys. Med. Biol.* **22**, 971–4.

Andrew, E. R., Bottomley, P. A., Hinshaw, W. S., Holland, G. N., Moore, W. S., Simaroj, C. & Worthington, B. S. 1979 NMR imaging in medicine and biology. *Proc. XX Ampere Congress* (*Tallinn, USSR*, 1978), pp. 53–56. Berlin: Springer-Verlag.

Andrew, E. R., Finney, A. & Mansfield, P. 1970 Investigation of pulse storage by nuclear magnetic resonance. *Royal Radar Establishemnt Res. Rep.* PD/24/026/AT.

Bloch, F. 1978 The early days of NMR. VIII Int. Conf. on magn. Reson. in Biological Systems (Nara, Japan). (Unpublished lecture.)

Bloch, F., Hansen, W. W. & Packard, M. E. 1946 The nuclear induction experiment. *Phys. Rev.* **70**, 474–485.

Bottomley, P. A. & Andrew, E. R. 1978 RF magnetic field penetration, phase shift and power dissipation in biological tissue: implications for NMR imaging. *Phys. Med. Biol.* **23**, 630-643.

Brooker, H. R. & Hinshaw, W. S., 1978 Thin section NMR imaging. *J. magn. Reson.* **30**, 129–131.

PHILOSOPHICAL TRANSACTIONS OF THE ROYAL SOCIETY B BIOLOGICAL SCIENCES

Brunner, P. & Ernst, R. R. 1979 Sensitivity and performance time in NMR imaging. *J. magn. Reson.* **33**, 83–106.
Damadian, R. 1972 Apparatus and methods for detecting cancer in tissue. *U.S. Patent* no. 3,789,832, filed 17 March 1972.
Damadian, R. 1971 Tumour detection by nuclear magnetic resonance. *Science, N.Y.* **171**, 1151–1153.
Damadian, R., Minkoff, L., Goldsmith, M., Stanford, M. & Koutcher, J. 1976 Tumour imaging in a live animal by field focussing NMR (FONAR). *Physiol. Chem. Phys.* **8**, 61–65.
Gabillard, R. 1951 Measurement of relaxation time T_2 in the presence of an inhomogeneous magnetic field. *C.r. hebd. Séanc. Acad. Sci., Paris* **232**, 1551–1553.
Gabillard, R. 1952 A steady state transient technique in nuclear resonance. *Phys. Rev.* **85**, 694–695.
Garroway, A. N. Grannell, P. K. & Mansfield, P. 1974 Image formation in NMR by a selective irradiative process. *J. Phys.* C **7**, L457–462.
Hahn, E. L. 1950 Spin echoes. *Phys. Rev.* **80**, 580–594.
Hinshaw, W. S. 1974*a* Spin mapping. *Phys. Lett.* A **48**, 87–88.
Hinshaw, W. S. 1974*b* The application of time dependent field gradients to NMR spin mapping. *Proc. XVIII Ampere Congress* (*Nottingham*) (ed. P. S. Allen, E. R. Andrew & C. A. Bates), pp. 433–434. Amsterdam: North-Holland.
Hinshaw, W. S. 1976 Image formation by nuclear magnetic resonance: the sensitive point method. *J. appl. Phys.* **47**, 3709–3721.
Hinshaw, W. S., Bottomley, P. A. & Holland, G. N. 1977 Radiographic thin section image of the human wrist by nuclear magnetic resonance. *Nature, Lond.* **270**, 722–723.
Hinshaw, W. S., Andrew, E. R., Bottomley, P. A., Holland, G. N., Moore, W. S. & Worthington, B. S., 1978*a* Display of cross-sectional anatomy by nuclear magnetic resonance imaging. *Br. J. Radiol.* **51**, 273–280.
Hinshaw, W. S., Andrew, E. R., Bottomley, P. A., Holland, G. N., Moore, W. S. & Worthington, B. S. 1978*b* Internal structural mapping by nuclear magnetic resonance. *Neuroradiology* **16**, 607–609.
Holland, G. N. & Bottomley, P. A. 1977 A colour display for NMR imaging. *J. Phys.* E **10**, 714–716.
Holland, G. N., Bottomley, P. A. & Hinshaw, W. S. 1977 ^{19}F magnetic resonance imaging. *J. magn. Reson.* **28**, 133–136.
Hoult, D. I. 1979 Rotating frame zeugmatography. *J. magn. Reson.*, **33**, 183–197.
Hounsfield, G. N. 1973 Computerized transverse axial scanning (tomography). *Br. J. Radiol.* **46**, 1016–1022.
Hutchison, J. M. S. 1976 Imaging by nuclear magnetic resonance. *Proc. 7th L. H. Gray Conference* (*Leeds*), pp. 135–141. Chichester: Wiley.
Kumar, A., Welti, D. & Ernst, R. R. 1975*a* Imaging of macroscopic objects by NMR Fourier zeugmatography. *Naturwissenschaften* **62**, 34.
Kumar, A., Welti, D. & Ernst, R. R. 1975*b* NMR Fourier zeugmatography. *J. magn. Reson.* **18**, 69–83.
Lauterbur, P. C. 1973 Image formation by induced local interactions: examples employing nuclear magnetic resonance. *Nature, Lond.* **242**, 190–191.
Lauterbur, P. C., Lai, C. M., Chen, C. N. & Kramer, D. 1977 Recent advances in imaging by magnetic resonance zeugmatography. Poster presented at Sixth International Symposium on Magnetic Resonance (Banff, Canada).
Lauterbur, P. C., Dulcey, C. S., Lai, C. M., Feiler, M. A., House, W. V., Kramer, D. M., Chen, C. N. & Dias, R. 1974 Magnetic resonance zeugmatography. *Proc. XVIII Ampere Congress* (*Nottingham*) (ed. P. S. Allen, E. R. Andrew & C. A. Bates), pp. 27–29. Amsterdam: North-Holland.
Lauterbur, P. C., Kramer, D. M., House, W. V. & Chen, C. N. 1975 Zeugmatographic high resolution nuclear magnetic resonance spectroscopy. Images of chemical inhomogeneity within macroscopic objects. *J. Am. chem. Soc.* **97**, 6866–6868.
Mansfield, P. 1976 Proton spin imaging by nuclear magnetic resonance. *Contemp. Phys.* **71**, 553–576.
Mansfield, P. 1977 Multiplanar image formation using NMR spin echoes. *J. Phys.* C **10**, L55–58.
Mansfield, P. & Grannell, P. K. 1973 NMR diffraction in solids? *J. Phys.* C **6**, L422–426.
Mansfield, P., Maudsley, A. A. & Baines, T. 1976 Fast scan proton density imaging by NMR, *J. Phys.* E **9**, 271–278.
Pullan, B. R. 1979 Computer tomography. *Medical imaging* (ed. L. Kreel), ch. 2, pp. 10–14. Aylesbury: H. M. and M. Publishers.
Pullan, B. R., Rutherford, R. A. & Isherwood, I. 1976 Computerized transaxial tomography. *Proc. 7th L. H. Gray Conference* (*Leeds*), pp. 20–37. Chichester: Wiley.

PHILOSOPHICAL TRANSACTIONS OF THE ROYAL SOCIETY B BIOLOGICAL SCIENCES

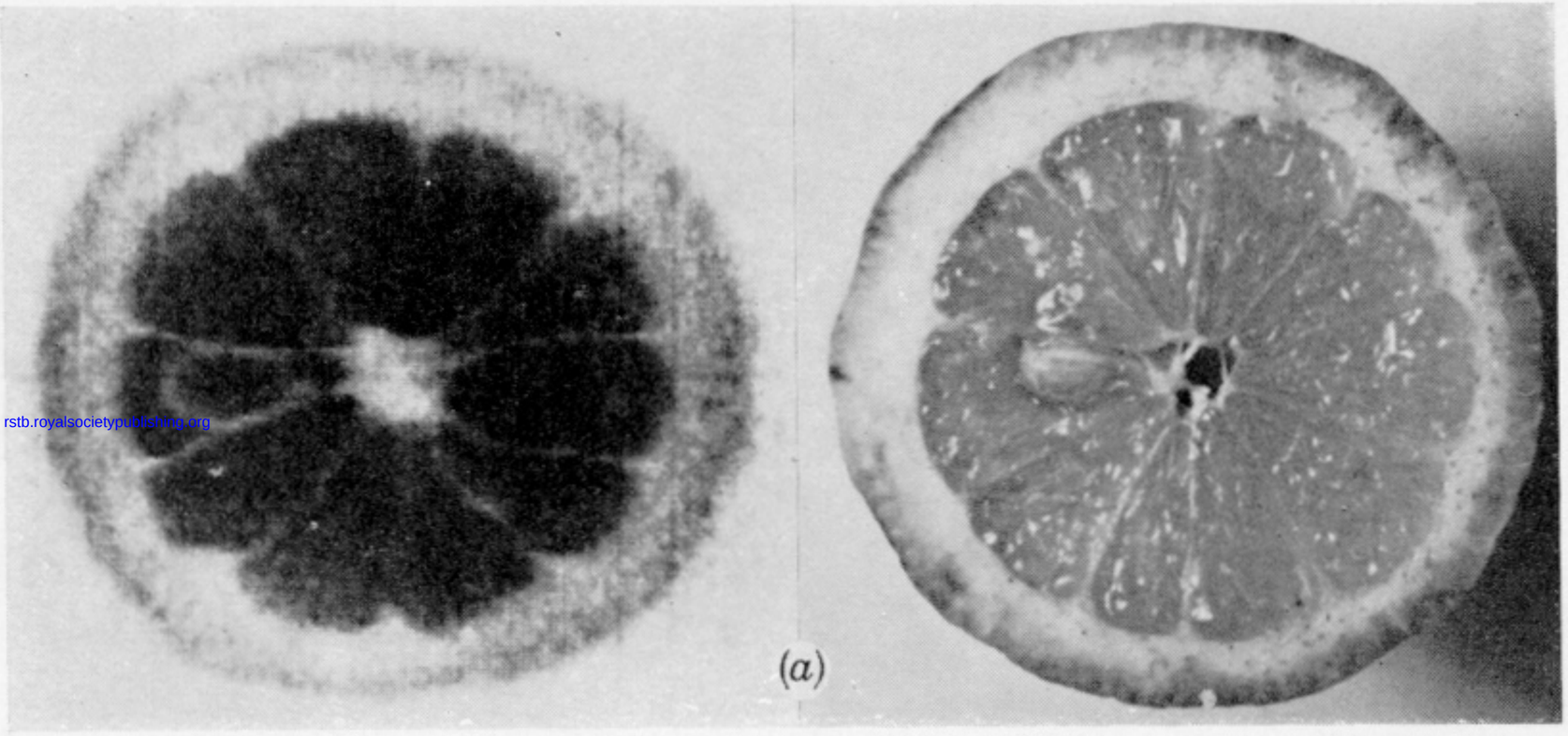

(a)

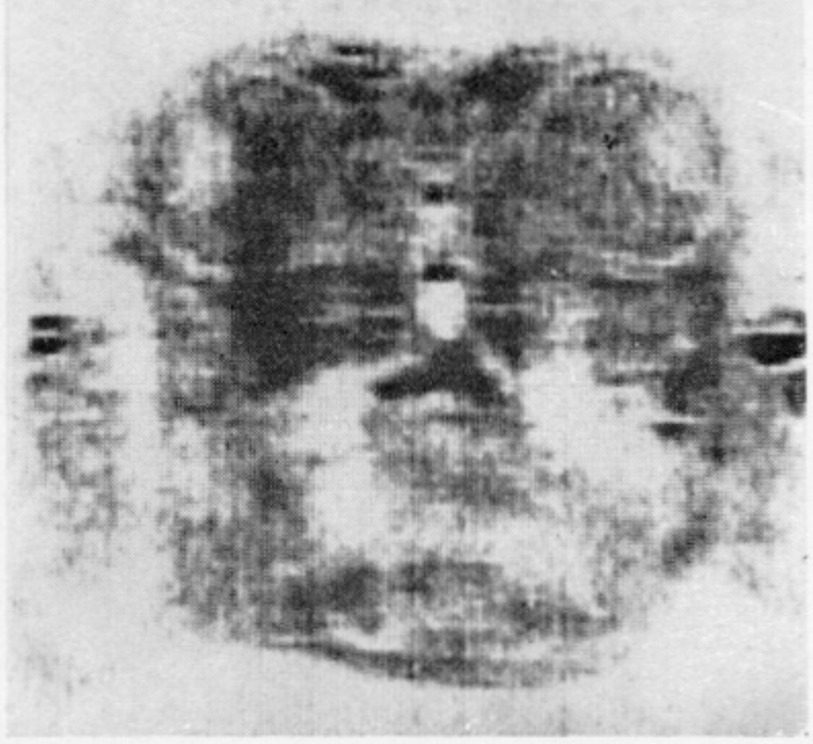

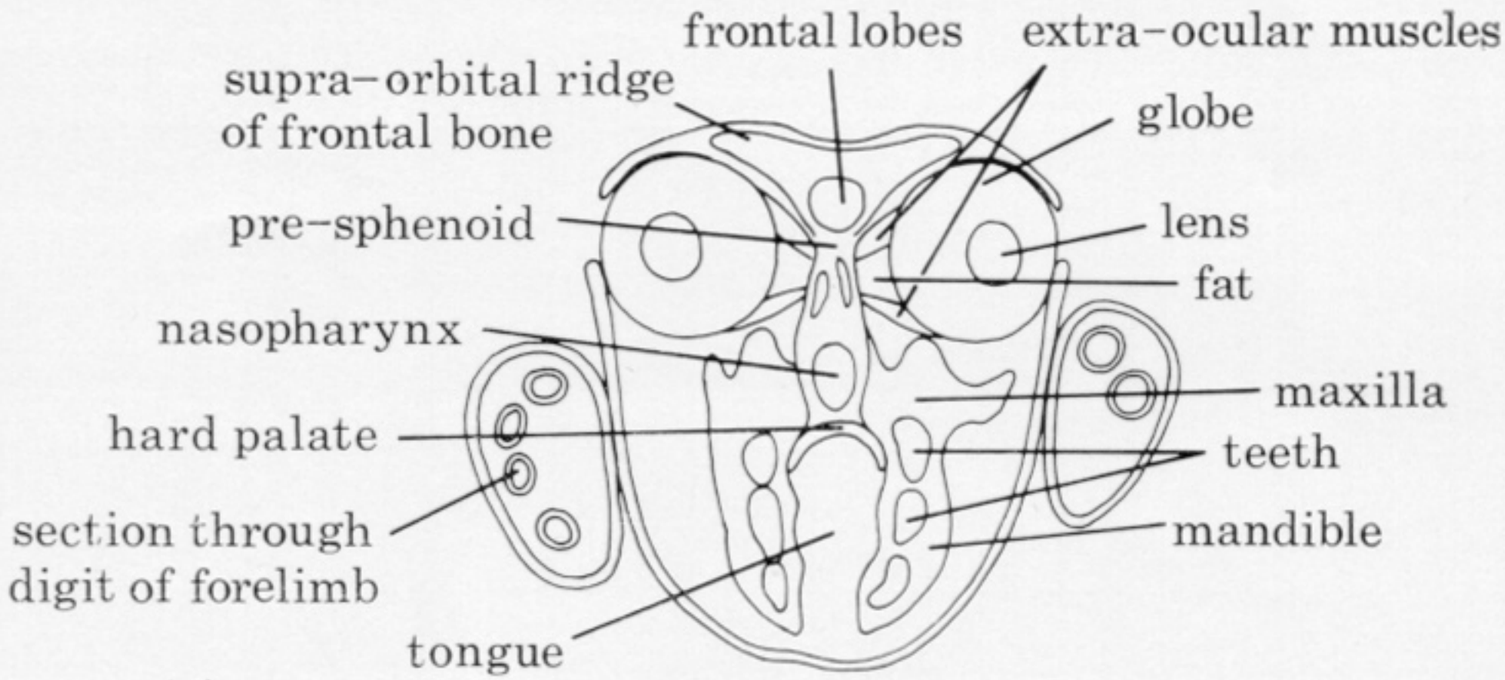

(b)

FIGURE 5. (*a*) Thin transverse section proton n.m.r. image of an intact lemon (left) and photograph of actual section cut subsequently (right). (*b*) Thin coronal section proton n.m.r. image through middle of orbits of rabbit's head (left) and annotated diagram indicating recognizable anatomical structure (right). Details of these images are given in the text. The images in plates 1 and 2 were obtained by an MRC supported group at Nottingham University consisting of E. R. Andrew, P. A. Bottomley, W. S. Hinshaw, G. N. Holland, W. S. Moore, C. Simaroj & B. S. Worthington.

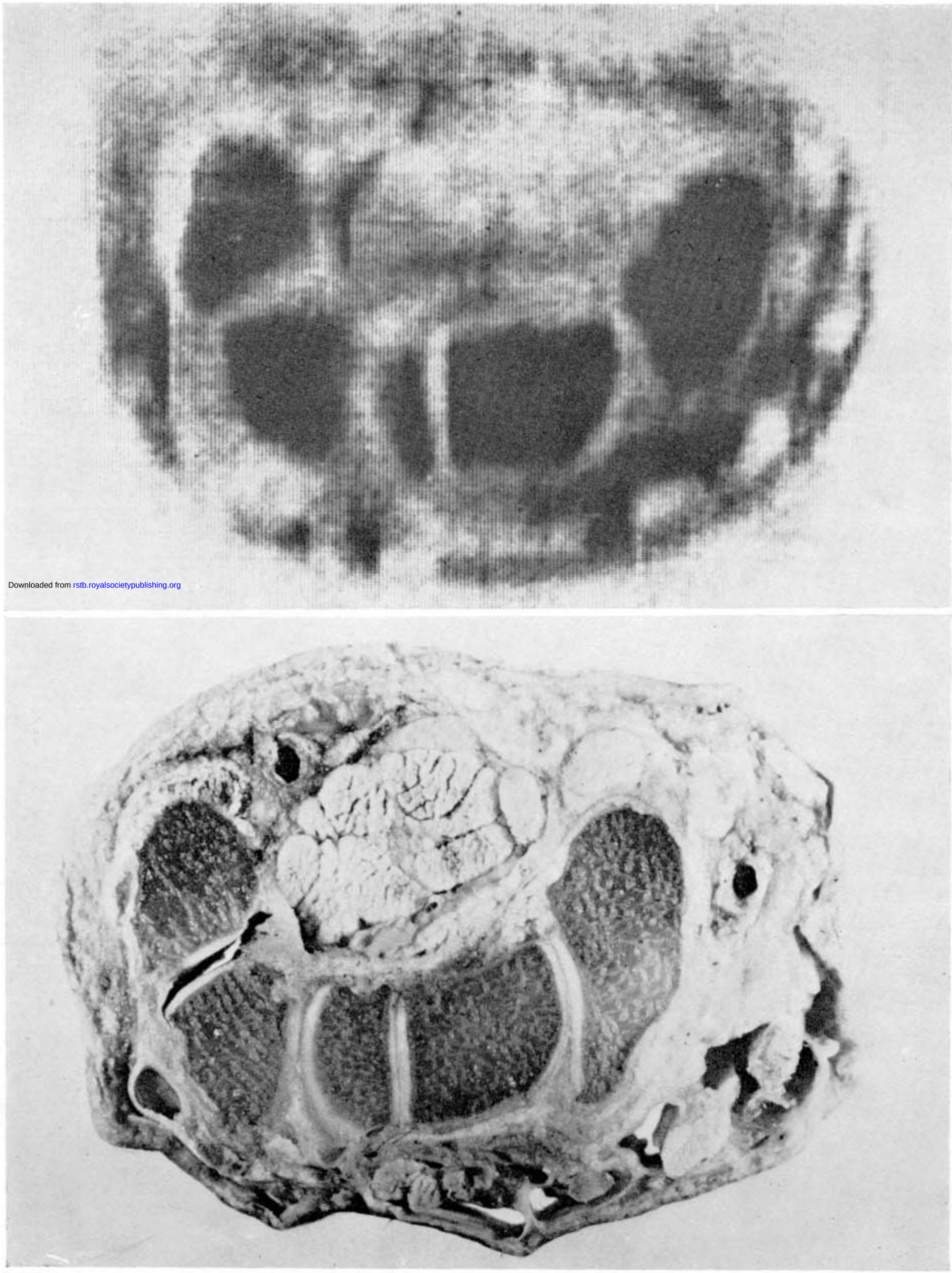

PHILOSOPHICAL TRANSACTIONS OF THE ROYAL SOCIETY B BIOLOGICAL SCIENCES

FIGURE 6. Thin transverse proton n.m.r. image through the left wrist of Dr P. Bottomley (above) and a photograph of a matching section from a cadaver wrist (below). Details of the image and the anatomical features observable are described in the text (Hinshaw *et al.* 1977, 1978*b*).